Distance-Based Ecological Driving Scheme Using a Two-Stage Hierarchy for Long-Term Optimization and Short-Term Adaptation

Hansang Lim, *Member, IEEE*, Wencong Su, *Member, IEEE*, and Chunting Chris Mi, *Fellow, IEEE*

***Abstract*—This paper proposes a distance-based ecological (eco)-driving scheme with two stages: one for long-term speed optimization and the other for short-term adaptation to actual traffic conditions. Before departure, the speed profile for an entire route is optimized in a distance domain by using characteristics of the drivetrain and road conditions. Then, while driving, the speed at only the next location is controlled to follow the optimal speed profile and adapt it for traffic conditions, which allows for real-time adaptation, maintaining optimal driving in the long term. To localize the change of the optimal speed profile due to traffic conditions, models for fuel rate of a conventional vehicle and vehicle propulsion systems were formulated in a distance domain, and a distance-based optimal speed profile was generated. The proposed eco-driving scheme is optimized by the quadratic programming method, and its validity is tested by simulation.**

***Index Terms*—Distance based, ecological (eco) driving, long-term optimization, short-term adaptation, traffic conditions.**

I. Introduction

ENERGY efficiency in a vehicle depends on not only the characteristics of its drivetrain but also on its operating conditions according to road and traffic conditions and driving patterns, which are consequently related to a vehicle's speed and acceleration. An ecological (eco)-driving system helps a vehicle operate in particular conditions with good energy efficiency by giving advice to drivers, generating an optimal speed profile, or controlling its driving.

For energy savings and environmental protection, many studies on eco driving have been reported. One issue is to assist drivers in driving a vehicle in energy-efficient ways. The optimal ways to accelerate and cruise are analyzed for diverse types of vehicles by simulations [1]. A specific guide is given to a driver under a particular vehicle loading [2], and by using the Global Positioning System and controller area network bus data, five types of detailed feedback are provided for eco driving [3]. An onboard driver-assistance system gives visual feedback and audible warning for uneconomical power demands [4].

Another issue is an eco-cruise control, which controls the driving speed automatically. An optimal vehicle control plan is generated by using anticipated roadway grade information, and the vehicle speed is varied within a preset speed window [5]. A model-predictive eco-cruise controller for serial electric vehicles is presented by using vehicle dynamics formulated in terms of position [6]. For real-time implementation, an eco-cruise controller is presented by using a quadratic cost function and a convex piecewise linear approximation of energy consumption maps in electric vehicles [7].

Recently, eco-driving research has focused on optimization of a driving speed profile. The main optimization approach for eco driving is the dynamic programming method [8]–[11] due to the nonlinear cost function with complex constraints. While dynamic programming can solve the global optimization of the speed profile over the entire driving route, it requires full knowledge of the driving conditions. Since it is hardly possible to anticipate exactly what is happening in advance, the optimal speed profile usually needs to be adapted for traffic conditions while driving. In particular, these approaches are based on a time domain, and the remaining profile, after any deviations from a time-based speed profile, needs to be fully optimized again. However, its computation time is too long to be implemented in real time; thus, this dynamic programming approach is not suited to online eco driving.

Common approaches for online eco driving reduce their computing times by carrying out optimization for a finite horizon of the route and repeating it at every time step. Model predictive controls (MPCs) are carried out for varying road and traffic conditions [12] or for roads with up–down gradients [13], which utilize the continuation and generalized minimum residual (C/GMRES) method. An MPC utilizing the quadratic programming (QP) method works in vehicle-to-vehicle communications [14]. The Legendre pseudospectral method, which converges quickly on an optimal solution, is applied for a finite horizon in hilly road conditions [15].

Toward comprehensive optimization, an approach to integration of future driving conditions and eco-driving systems has been adopted. The velocity profile is periodically determined by highway traffic data, which come from the California Freeway Performance Measurement System (PeMS) [16], [17], and an MPC computes an optimal engine torque using the determined

Manuscript received November 8, 2015; revised May 3, 2016; accepted May 20, 2016. Date of publication June 14, 2016; date of current version March 10, 2017. The review of this paper was coordinated by Dr. D. Cao.

H. Lim is with the Department of Electronics Convergence Engineering, Kwangwoon University, Seoul 139-701, South Korea, and also with the Department of Electrical and Computer Engineering, University of Michigan–Dearborn, Dearborn, MI 48128 USA (e-mail: lhs@kw.ac.kr).

W. Su is with the Department of Electrical and Computer Engineering, University of Michigan–Dearborn, Dearborn, MI 48128 USA (e-mail: wencong@umich.edu).

C. C. Mi is with the Department of Electrical and Computer Engineering, San Diego State University, San Diego, CA 92182 USA (e-mail: cmi@sdsu.edu).

Color versions of one or more of the figures in this paper are available online at http://ieeexplore.ieee.org.

Digital Object Identifier 10.1109/TVT.2016.2574643

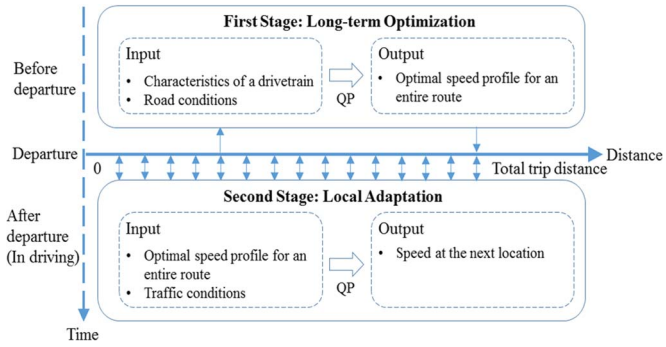

Fig. 1. Proposed distance-based eco-driving scheme with two stages.

velocity profile [18]. With known or measured information of the current road and traffic signals, the future states of the preceding vehicle are predicted, and the optimal control input is computed by C/GMRES [19]. For reducing stops at traffic lights, the state of the traffic lights is mathematically formulated, and the optimal velocity trajectory is advised [20].

These approaches deal with only a partial horizon, not an entire one, which makes their optimization results largely dependent on the horizon length [18]. While a long horizon with reliable prediction data improves fuel economy satisfactorily, it requires a much longer computing time, which is critical for real-time implementation of online eco driving, and accurate traffic conditions for a long horizon. A short horizon, more suitable for real-time computation, generally generates a speed profile less optimized for an entire route or the long term. In addition, traffic conditions also affect the optimal horizon length. Thus, the primary challenge in online eco driving is to obtain satisfactory optimization results in the long term with a fast enough computing time to be implemented in real time.

In this paper, a distance-based eco-driving scheme using a two-stage hierarchy is presented to overcome this challenge. Fig. 1 shows its overall structure. The first stage is for a long-term optimization before departure, usually for an entire driving route without consideration of traffic conditions, and the second is its local adaptation to traffic conditions while driving. In particular, the optimization is made in a distance domain instead of a time domain to limit the adapted regions to nearby regions directly undergoing heavy traffic, which can keep the effectiveness of the long-term optimization and avoid reoptimizing the speed profile for the remaining trip.

A two-stage framework has been used in some applications such as energy management in plug-in or hybrid electric vehicles (P/HEVs) [21]–[23] and economic operation of renewable energy generation [24]. However, energy management in P/HEVs and renewable energy generation are different from eco-driving control for internal combustion engine (ICE)-based vehicles. They have different plant architectures, including different dynamic models and power sources, which leads to different control and state variables and objective functions. Above all, they formulate the models and cost functions in a time domain and optimize the control problems in a time domain, not a distance domain [21]–[24]. After a vehicle undergoes a heavy traffic condition, the actual time steps deviate from the time steps of the optimal speed profile obtained from the first stage. Therefore, the speed profile optimized in a time domain cannot act as a reference and keep its effectiveness. Eco-cruise control for electric vehicles and energy management for electric ground vehicles formulated in a distance domain [6], [26] cannot adapt to actual traffic conditions without a hierarchical framework.

The main contributions of this paper are as follows. First, a distance-based eco-driving scheme with two stages is proposed. The proposed distance-based two-stage scheme can keep the effectiveness of the long-term optimal speed profile since the speed profile still acts as a reference, except in areas under heavy traffic conditions. Second, vehicle models and the cost function are formulated in a distance domain, and a distance-based speed profile is generated to support the scheme. Finally, the cost functions for the two stages are formulated into a quadratic matrix form with linear constraints suitable for efficient solvers with guaranteed convergence.

This paper is organized as follows. In Section II, models for fuel rate and vehicle propulsion are formulated. Section III presents the concept of the proposed eco-driving scheme, and the cost function for optimization is described for each stage. In Section IV, simulation results are analyzed, and discussions and conclusions are given in Section V.

II. Vehicle Model for Control

To estimate the fuel consumption, a fuel rate model is formulated for an automatic transmission midsize vehicle by using performance data obtained from Autonomie software [27]. Then, the longitudinal dynamics of a vehicle are formulated, and the state equation between the current and next speeds is derived.

Autonomie is a simulation tool for vehicle energy consumption and performance analysis developed by Argonne National Laboratory in collaboration with automotive manufacturers and sponsored by the U.S. Department of Energy. It is a MATLAB-based software environment and framework and supports a wide range of vehicle classes and powertrain configurations such as ICE-based vehicles, HEVs, PHEVs, and battery electric vehicles. The models of Autonomie have been validated against the Toyota Prius [28] and the General Motors Volt [29].

A. Fuel Rate Model

To make the computation time for optimization short, a model based on the Willans line approximation [30] is formulated. The left panel in Fig. 2 is the engine Willans plot given by Autonomie, which shows a piecewise linear relation between the fuel rate $\dot{m}_f$ and the engine torque T_e, for a fixed engine speed ω, so that the fuel rate for a given engine speed can be written as

$$\dot{m}_f = f(T_e|\omega) = \begin{cases} k_1(\omega)T_e + c_1(\omega), & \text{for } T_e \geq 0 \\ k_2(\omega)T_e + c_2(\omega), & \text{for } T_e < 0. \end{cases} \quad (1)$$

The right panel in Fig. 2 shows that the fuel rate for $T_e \geq 0$, which is a region of interest, is linearly proportional to the engine speed for a fixed torque. Thus, $k_1(\omega)$ and $c_1(\omega)$ can be

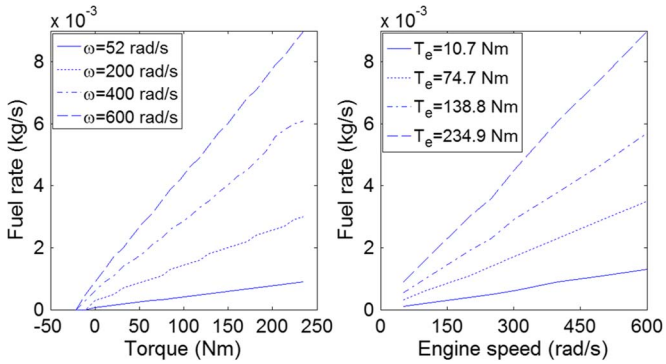

Fig. 2. Relationship between fuel rate, torque, and engine speed.

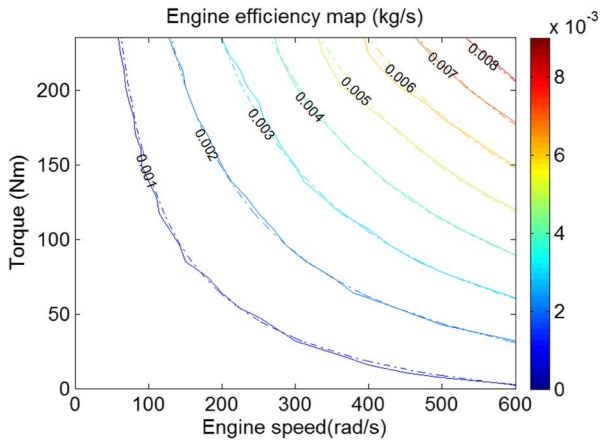

Fig. 3. Comparison of fuel maps.

represented by a linear function of the engine speed. Therefore, the fuel rate can be modeled by

$$\begin{aligned}\dot{m}_f = f(T_e,\omega) &= (\beta_1\omega+\beta_2)T_e+\gamma_1\omega+\gamma_2\\ &= (\beta_1 T_e+\gamma_1)\omega+\beta_2 T_e+\gamma_2 \end{aligned} \quad (2)$$

where $\beta_1 = 5.646\times10^{-8}$, $\beta_2 = 4.751\times10^{-7}$, $\gamma_1 = 1.625\times10^{-6}$, and $\gamma_2 = -5.968\times10^{-5}$.

This fuel rate model is evaluated by comparing the fuel map estimated by the model with the fuel map generated by Autonomie. The comparison is shown in Fig. 3. The solid and dashed lines represent the Autonomie and model data, respectively. This comparison shows that the model is acceptable for estimation of the fuel consumption.

B. Vehicle Propulsion Model

In the longitudinal motion of a vehicle, a wheel force F_w for propelling a vehicle is

$$\begin{aligned}F_w(t) = \frac{T_w(t)}{r_w} &= \frac{f_r g_r(n) N_{\rm fr} N_{\rm gr}(n)}{r_w} T_e(t)\\ &= m\dot{v}(t)+\frac{1}{2}\rho C_d A_d v(t)^2 + mgC_r\cos\theta(t)\\ &\quad + mg\sin\theta(t) + F_{\rm brake}(t)\end{aligned} \quad (3)$$

where T_w is a wheel torque (N · m), and T_e is an engine torque (N · m). Then, $v(t)$, $\dot{v}(t)$, $\theta(t)$, and $F_{\rm brake}(t)$ are the speed of the vehicle (m/s), its acceleration (m/s^2), the road gradient (rad), and the brake force (N), respectively. The other parameters of the vehicle model and their values are given in Table I.

TABLE I
PARAMETERS OF THE VEHICLE MODEL

Symbol	Quantity	Value	Unit
m	Mass	1607	kg
f_r	Final drive ratio	4.438	-
$g_r(n)$	Gear ratio for a given gear number n	2.563,1.552,1.022, 0.727,0.52	-
N_{fr}	Efficiency of a final drive	0.97	-
$N_{gr}(n)$	Efficiency of a gear box and a torque converter	-	-
r_w	Wheel radius	0.30115	m
ρ	Air density	1.19854	kg/m^3
C_d	Air drag coefficient	0.3	-
A_d	Frontal area	2.25084	m^2
C_r	Rolling resistance coefficient	-	-
g	gravity	9.81	m/s^2

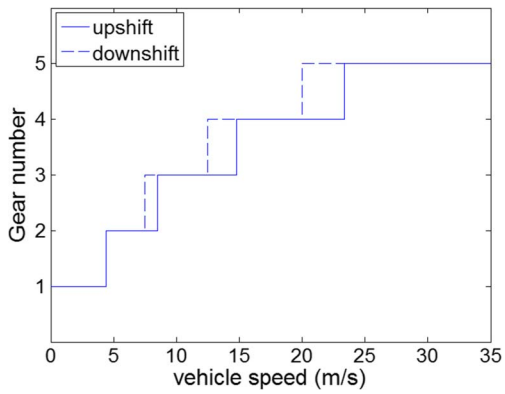

Fig. 4. Gear shift model.

The gear number is assumed to be controlled by only the speed and the direction of the acceleration, as shown in Fig. 4. The rolling resistance coefficient C_r is modeled by a linear function of the engine speed. The efficiency of the final drive is modeled to be a constant. $N_{\rm gr}(n)$ is a function of the gear number, an input speed, and an input torque and modeled as the product of the gearbox efficiency and the torque converter efficiency. Since the efficiency of a gearbox for a fixed gear number is almost constant, except at very low engine speeds, it is modeled as a constant whose value is dependent on only the gear number.

The efficiency of a torque converter shows more dependence on the operating conditions, as shown in Fig. 5. The dependence of the efficiency on varying input speeds for a fixed input torque is estimated by a quadratic model, and its dependence on varying input torques at a fixed input speed is modeled as a piecewise linear equation as follows:

$$\begin{aligned}g(T,\omega) = \min(&d_1(\omega)T+d_2(\omega), e_1(\omega)T+e_2(\omega),\\ &f_1(\omega)T+f_2(\omega))\end{aligned} \quad (4)$$

where $d_i(\omega)$, $e_i(\omega)$, and $f_i(\omega)$ are quadratic functions of the input speeds. The circles in Fig. 5 represent the efficiency data obtained from Autonomie, and the solid, dotted, and dashed lines represent the data given by the model. They are in good agreement. Other parameters, except functions of time such as $T_e(t)$, $F_{\rm brake}(t)$, $v(t)$, $\dot{v}(t)$, and $\theta(t)$, are modeled by constants.

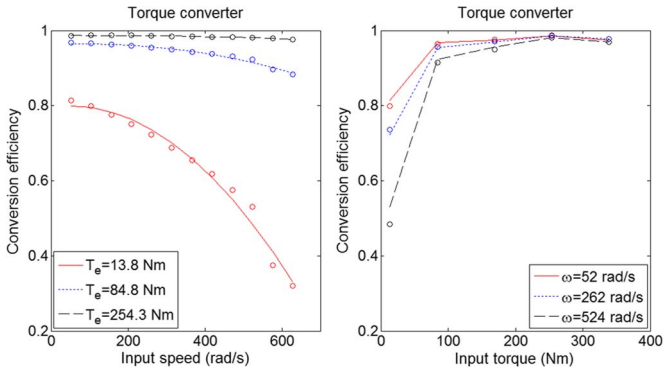

Fig. 5. Efficiency of a torque converter.

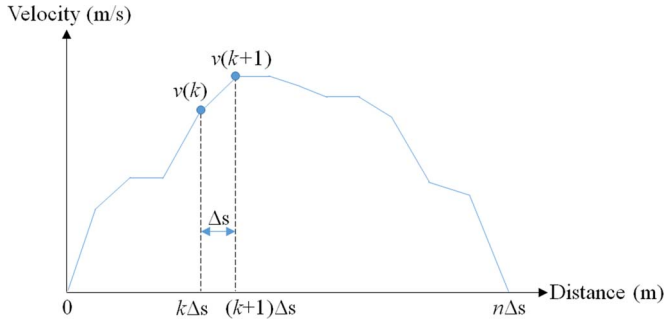

Fig. 6. Distance-based speed profile.

From (3), the acceleration can be derived by

$$\dot{v}(t) = \frac{1}{m}\left(\frac{f_r g_r(n) N_{\mathrm{fr}} N_{\mathrm{gr}}(n)}{r_w} T_e(t) - \frac{1}{2}\rho C_d A_d v(t)^2 - mgC_r \cos\theta(t) - mg\sin\theta(t) - F_{\mathrm{brake}}(t)\right). \quad (5)$$

In (5), $T_e(t)$ and $F_{\mathrm{brake}}(t)$ are the control inputs, which determine the acceleration and deceleration and, consequently, the fuel consumption.

Then, the speed at the next time step, which is the result of the control inputs, is given by

$$\begin{aligned} v(t+\Delta t_k) &= v(t) + \dot{v}(t)\Delta t_k \\ &= \left(1 - \frac{C_2}{m} v(t)\Delta t_k\right) v(t) \\ &\quad + \left[\tfrac{C_1}{m}\Delta t_k, \ -\tfrac{1}{m}\Delta t_k\right] \begin{bmatrix} T_e(t) \\ F_{\mathrm{brake}}(t) \end{bmatrix} - \frac{C_3}{m}\Delta t_k \end{aligned} \quad (6)$$

where Δt_k is the time interval between adjacent steps, $C_1 = f_r g_r(n) N_{\mathrm{fr}} N_{\mathrm{gr}}(n)/r_w$, $C_2 = (1/2)\rho C_d A_d$, and $C_3 = mgC_r \cos\theta(t) + mg\sin\theta(t)$.

III. Distance-Based Eco-Driving Scheme With a Two-Stage Hierarchy

To generate a speed profile that guarantees long-term optimization and to adapt it for real-time traffic conditions, a distance-based eco-driving scheme with two stages is proposed. The structure of the proposed eco-driving scheme and its two stages, i.e., the long-term optimization and the local adaptation, are described.

A. Fundamental Concept

Before departure, the first stage generates an optimal speed profile for an entire driving route in a distance domain by using characteristics of the drivetrain and road conditions, such as road gradients, trip distance, and speed limits. Traffic conditions are not taken into consideration. The QP method is used as an optimization algorithm since it is one of the most widely used optimization methods for global optimization [14], [31], [32] and requires much shorter computation time than dynamic programming [8]–[11], [33]. Thus, the generated speed profile, which is called a reference speed profile, guarantees long-term optimization in ideal traffic conditions, i.e., very smooth traffic.

After departure, the second stage controls the vehicle speed by taking the reference speed profile and traffic conditions into account. This control is carried out for the vehicle speed at only the next location, which makes the computation time short enough to be suitable for real-time implementation. Spacing to the preceding vehicle is used as a traffic condition index. The spacing at the next location is estimated by using the previous acceleration of the preceding vehicle. Under smooth traffic conditions, the spacing to the preceding vehicle is farther than the safety spacing required at the current speed, and the vehicle is controlled to be driving at the reference speed; however, if the spacing is closer than the required spacing under heavy traffic conditions, the speed value to secure the required safety spacing is computed, and the speed at the next location is set to a value that is slower than the reference speed. After passing heavy traffic regions, the vehicle follows the reference speed again.

In a time-based driving cycle, any adaptation of the reference speed profile to traffic conditions changes the entire driving time, which changes the whole speed profile after that adaptation, although the adapted time period is very short compared with the entire driving time. Consequently, it is required to compute the optimal speed profile for the remaining route again, which is a major disadvantage to online eco driving, since its computation time is long and traffic conditions usually continue to change.

On the other hand, in a distance-based driving cycle, the speed profile is only changed for nearby locations that are directly affected by traffic conditions, since the characteristics of the drivetrain and road conditions are not changed during driving. Thus, the change of the speed profile due to traffic conditions is localized, and the reference speed profile can still be effective in other locations. Long-term optimization can be maintained if the regions under heavy traffic conditions are not too wide and if the driving route does not include too many traffic signals. That is the reason why we optimize the speed profile in a distance domain.

A distance-based speed profile is shown in Fig. 6. In a distance domain, each location has the same distance of Δs, and the control inputs are updated with a fixed distance step. If the total number of distance steps is n, the trip distance S is

$$S = n\Delta s. \quad (7)$$

The acceleration is assumed to be a constant within each distance step.

Let the speed and the driving distance at the location of $k\Delta s$ be $v(k)$ and $S(k)$, respectively. The driving distance at the location of $(k+1)\Delta s$ is given by

$$\begin{aligned} S(k+1) &= S(k) + \int_{t_k}^{t_{k+1}} v(k) + \dot{v}(k)(t-t_k)dt \\ &= S(k) + v(k)(t_{k+1}-t_k) + \frac{1}{2}\dot{v}(k)(t_{k+1}-t_k)^2 \end{aligned} \quad (8)$$

where t_{k+1} and t_k are the times at the locations of $(k+1)\Delta s$ and $k\Delta s$, respectively.

Therefore, the distance step can be written as

$$\begin{aligned} \Delta s &= S(k+1) - S(k) \\ &= v(k)\Delta t_k + \frac{1}{2}\dot{v}(k)\Delta {t_k}^2 = \frac{v(k)+v(k+1)}{2}\Delta t_k \end{aligned} \quad (9)$$

where $\Delta t_k = t_{k+1} - t_k$, and from (9), the time interval is derived by

$$\Delta t_k = \frac{2\Delta s}{v(k)+v(k+1)}. \quad (10)$$

By inserting (10) into (6) and multiplying both sides by "$v(k)+v(k+1)$," the state equation for the speed in a distance domain is described by

$$\begin{aligned} v(k+1)^2 = &\left(1 - \frac{2C_2\Delta s}{m}\right) v(k)^2 \\ &+ \left[\tfrac{2C_1\Delta s}{m}, \quad -\tfrac{2\Delta s}{m}\right] \begin{bmatrix} T_e(k) \\ F_{\text{brake}}(k) \end{bmatrix} - \frac{2C_3\Delta s}{m} \end{aligned} \quad (11)$$

and by replacing $v(k)^2$ with $X(k)$ and setting the control inputs $u(k) = [T_e(k), F_{\text{brake}}(k)]^T$, (11) can be described by

$$X(k+1) = A(k)X(k) + B(k)u(k) - D(k) \quad (12)$$

where $A(k) = (1-(2C_2\Delta s/m))$, $B(k) = [2C_1\Delta s/m, -(2\Delta s/m)]$, and $D(k) = 2C_3\Delta s/m$.

Then, from (12), the vehicle longitudinal states for all distance steps can be represented by (13), shown at the bottom of the page.

B. Long-Term Optimization

The optimal speed profile for an entire driving route is generated, which guarantees a good balance between fuel consumption and driving time in the long term and acts as a reference speed, which a vehicle will follow while driving. The trip distance, road gradients, and speed limits are inputted as road conditions.

Although this long-term optimization is performed before departure and does not require a real-time computation, the allowable computation time is limited. Thus, the QP method is used for optimization, since it can save computation time, as opposed to the dynamic programming method.

If only the fuel consumption is considered, a speed profile with a low speed and a long driving time will be generated, which is not practical. Thus, by taking the fuel consumption and the driving time into consideration, the cost function is written as

$$J = w_1 \sum_{k=0}^{n-1} \dot{m}_f(k)\Delta t_k + w_2 \sum_{k=0}^{n-1} \left(v(k+1)^2 - V_{\text{target}}(k+1)^2\right)^2. \quad (14)$$

On the right side of the equation, the first and second terms represent the fuel consumption and the speed deviation from the target speed $V_{\text{target}}(k)$ at each location, respectively. A speed limit at each location is used as a target speed in this study. If available, the current or the historic speed data on constituent roads just before departure [16], [17], [21], [26] can be used, which reduces changes to the optimization results due to traffic conditions while driving. The second term makes the vehicle speed be close enough to the target speed and, consequently, prevents the driving time from being too long.

Constants w_1 and w_2 are weights for balancing the effect of the two terms. The speed, which is much lower than the speed limit on each route, consumes less fuel but is not applicable to an actual drive since the vehicle running at such a speed obstructs traffic. Thus, the values of w_1 and w_2 are chosen to set the vehicle's steady-state speed to be approximately the speed limit if the route is not too short to accelerate to the speed limit. By simplifying the time interval into $\Delta t_k \approx \Delta s/v(k)$ and replacing the engine speed with the vehicle speed, (14) is rewritten as (15), shown at the bottom of the next page.

$$\begin{aligned} X = \begin{bmatrix} X(0) \\ X(1) \\ \vdots \\ X(n-2) \\ X(n-1) \end{bmatrix} &= \begin{bmatrix} 1 \\ A(0) \\ \vdots \\ A(n-3)\cdots A(0) \\ A(n-2)\cdots A(0) \end{bmatrix} X(0) + \begin{bmatrix} 0 & 0 & \cdots & 0 & 0 \\ B(0) & 0 & \cdots & 0 & 0 \\ A(1)B(0) & B(1) & \cdots & 0 & 0 \\ & \vdots & & & \\ A(n-2)\cdots A(1)B(0) & A(n-2)\cdots A(2)B(1) & \cdots & B(n-2) & 0 \end{bmatrix} \\ &\times \begin{bmatrix} T_e(0) \\ F_{\text{brake}}(0) \\ \vdots \\ T_e(n-1) \\ F_{\text{brake}}(n-1) \end{bmatrix} + \begin{bmatrix} 0 & 0 & \cdots & 0 & 0 \\ 1 & 0 & \cdots & 0 & 0 \\ & \vdots & & & \\ A(n-3)\cdots A(1) & A(n-3)\cdots A(2) & \cdots & 0 & 0 \\ A(n-2)\cdots A(1) & A(n-2)\cdots A(2) & \cdots & 1 & 0 \end{bmatrix} \begin{bmatrix} D(0) \\ D(1) \\ \vdots \\ D(n-2) \\ D(n-1) \end{bmatrix} \\ &= \bar{A}X(0) + \bar{B}U + \bar{C}D \end{aligned} \quad (13)$$

Equation (15) is further simplified to apply the QP method. Since a constant term has no effect on optimization, $w_2 V_{\text{target}}(k+1)^4$ is not taken into consideration. The $\beta_2 T_e(k)$ and γ_2 terms are y-axis intercepts in the fuel map shown in the right panel in Fig. 2. The maximum variation in intercept values due to the engine torque is approximately 1×10^{-4}, which is one several tenths of the usual fuel rates and is negligible. Since $\gamma_1(f_r g_r(n)/r_w)$ shows a smaller variation due to the input control than $\beta_1(f_r g_r(n)/r_w)T_e$, this term is also neglected.

In addition, since $v(0) = v(n) = 0$, $\sum_{k=0}^{n-1} v(k+1)^2 = \sum_{k=0}^{n-1} v(k)^2$, and the simplified cost function is given by

$$\begin{aligned} J \approx \sum_{k=0}^{n-1} \Bigg(& w_2 v(k+1)^4 - 2w_2 V_{\text{target}}(k+1)^2 v(k+1)^2 \\ & + w_1 \beta_1 \frac{f_r g_r(n)}{r_w} \Delta s T_e(k) \Bigg) \\ = {} & w_2 X^T X - 2w_2 V_{\text{target}} X + KU \end{aligned} \tag{16}$$

where $V_{\text{target}} = \begin{bmatrix} V_{\text{target}}(0)^2 & \cdots & V_{\text{target}}(n-1)^2 \end{bmatrix}$, and $K = \begin{bmatrix} w_1\beta_1(f_r g_r(n)/r_w)\Delta s & 0 & \cdots & w_1\beta_1(f_r g_r(n)/r_w)\Delta s & 0 \end{bmatrix}$.

By applying (13) into (16) and simplifying the equation to be suitable for the QP method, the cost function is summarized by

$$\begin{aligned} J = {} & w_2 U^T \bar{B}^T \bar{B} U + [2w_2 X(0) \bar{A}^T \bar{B} + 2w_2 D^T \bar{C}^T \bar{B} \\ & - 2w_2 V_{\text{target}} \bar{B} + K] U \end{aligned} \tag{17}$$

subject to

$$\begin{aligned} \begin{bmatrix} 0 \\ 0 \end{bmatrix} \le u(k) = \begin{bmatrix} T_e(k) \\ F_{\text{brake}}(k) \end{bmatrix} \le \begin{bmatrix} T_{\max} \\ F_{\text{Brake(max)}} \end{bmatrix} \\ \omega_{\min} \le \omega(k) \le \omega_{\max} \\ v(k) \le \text{speed limit}(k) \\ v(0) = v(n) = 0 \end{aligned} \tag{18}$$

where the subscripts of min and max denote the minimum and maximum bounds, $\omega(k)$ is the engine speed at the kth location, speed limit(k) is the maximum speed of the kth location, $v(0)$ is the initial speed, n is the total number of steps, and $v(n)$ is the final speed of the entire route. Next, the optimization is performed by finding the control input pairs that minimize the cost function for a sufficiently long-term driving route, usually an entire route. Then, the optimal speed profile for an entire route is obtained by applying the resulting control input pairs to (13).

C. Local Adaptation for Traffic Conditions

After departure, the vehicle is driven to follow the reference speed profile. However, in actual driving, the reference speed profile cannot usually be followed, since it cannot reflect current traffic conditions. If there are numerous vehicles on the road, the spacing to the preceding vehicle, i.e., ΔL, tends to be shortened, and traffic conditions can be indicated by the spacing. For safety reasons, the spacing should be kept wider than a specific value, which is called the safety spacing. Thus, the speed needs to be adapted for traffic conditions while driving.

By using previous and current speeds of the preceding vehicle and the current spacing to the preceding vehicle, the next spacing is estimated. Then, the vehicle speed is adapted to keep the next spacing wider than the safety spacing if the reference speed does not ensure the safety spacing.

Let the acceleration, speed, and location of the preceding vehicle be $a_{\text{pre}}(\cdot)$, $v_{\text{pre}}(\cdot)$, and $L_{\text{pre}}(\cdot)$, respectively. $L(\cdot)$ represents the location of the driver's vehicle, and $\Delta L(\cdot)$ represents the spacing between the preceding vehicle and the driver's vehicle.

Assuming that the acceleration of the preceding vehicle is kept constant, its speed at the next location is estimated by

$$v_{\text{pre}}(k+1)^* \approx v_{\text{pre}}(k) + a_{\text{pre}}(k-1)\frac{\Delta s}{v(k-1)} \tag{19}$$

and its next location is estimated by

$$L_{\text{pre}}(k+1)^* \approx L_{\text{pre}}(k) + \frac{v_{\text{pre}}(k) + v_{\text{pre}}(k+1)^*}{2}\frac{\Delta s}{v(k)} \tag{20}$$

where the superscript $*$ represents the estimation value.

Then, the spacing at the next location can be estimated by

$$\begin{aligned} \Delta L(k+1)^* & \approx L_{\text{pre}}(k+1)^* - L(k+1) \\ & \approx \Delta L(k) + \left(\frac{v_{\text{pre}}(k) + v_{\text{pre}}(k+1)^*}{2}\frac{\Delta s}{v(k)} - \Delta s \right). \end{aligned} \tag{21}$$

The safety spacing is linearly modeled on the speed, as described in

$$\Delta L_S(k+1) = h \times v(k+1) + l \tag{22}$$

where h is a proportional constant whose value is set to 2 according to [10], and l represents a desired spacing to the preceding vehicle at the stop location, of which the value is set to 2.

$$J \approx \sum_{k=0}^{n-1} \left(w_1 \left((\beta_1 \frac{f_r g_r(n)}{r_w} v(k) + \beta_2) T_e(k) + \gamma_1 \frac{f_r g_r(n)}{r_w} v(k) + \gamma_2 \right) \frac{\Delta s}{v(k)} + w_2 \Big(v(k+1)^2 - V_{\text{target}}(k+1)^2 \Big)^2 \right) \tag{15}$$

To assure the safety spacing at the next location, the next speed is limited by

$$\Delta L(k+1)^* \geq \Delta L_S(k+1) = h \times v(k+1) + l$$
$$\therefore v(k+1) \leq \frac{\Delta L(k+1)^* - l}{h}. \tag{23}$$

Then, the speed is adapted by taking the spacing to the preceding vehicle, as well as the fuel efficiency and the speed deviation, into consideration. Since the optimal performance in the long term is maintained by the reference speed profile, the speed at only the next location is adapted at each location. The safety spacing should be ensured so that it is implemented by the boundary condition [14].

Thus, the cost function at each step has the same form as (17), except that computation is performed at only one location, and is given by

$$J = w_2 u(k)^T B(k)^T B(k) u(k) + [2w_2 X(k) A(k)^T B(k) + 2w_2 D(k)^T B(k) - 2w_2 V_{\text{target}}(k+1)^2 B(k) + K] u(k) \tag{24}$$

subject to

$$\begin{bmatrix} 0 \\ 0 \end{bmatrix} \leq u(k) = \begin{bmatrix} T_e(k) \\ F_{\text{brake}}(k) \end{bmatrix} \leq \begin{bmatrix} T_{\max} \\ F_{\text{Brake(max)}} \end{bmatrix}$$
$$\omega_{\min} \leq \omega(k) \leq \omega_{\max}$$
$$v(k) \leq \text{speed limit}(k)$$
$$v(k+1) \leq \frac{\Delta L(k+1)^* - l}{h} \tag{25}$$

where $V_{\text{target}}(k+1)$ represents not the speed limit but the reference speed obtained from the long-term optimization, and $K = \begin{bmatrix} w_1 \beta_1 (f_r g_r(n)/r_w) \Delta s & 0 \end{bmatrix}$ at the current speed. The QP method is used for minimizing the cost function, and computation for only one location makes this adaptation fast enough to be suitable for real-time applications.

IV. Simulations

The proposed eco-driving scheme is implemented and solved using MATLAB toolbox. A series of simulations were conducted by changing two weight values, namely, w_1 and w_2, and varying the speed of the preceding vehicle. Then, simulation results were compared with optimization results produced by the original, not simplified, cost function for validation.

The parameter values used in the simulations are as follows: $T_{\max} = 220$ N · m, and $F_{\text{Brake(max)}} = 3120$ N · m, where $F_{\text{Brake(max)}}$ is set to be half of the actual maximum brake force to avoid deceleration that is too hard.

A. Long-Term Optimization

A driving route under test is 5 km long and is hat-shaped with a speed limit of 60 and 80 km/h. A distance step Δs is set to be 25 m, and consequently, the total number of distance steps is 200.

TABLE II
Optimization Results for the Original Cost Function

	Weight Values ($w_{1(\text{norm})} = 10$)				
	$w_2 = 0.1$	$w_2 = 0.5$	$w_2 = 1$	$w_2 = 2$	$w_2 = 5$
Fuel (kg)	0.220	0.241	0.246	0.255	0.262
Time (s)	470	327	315	288	278

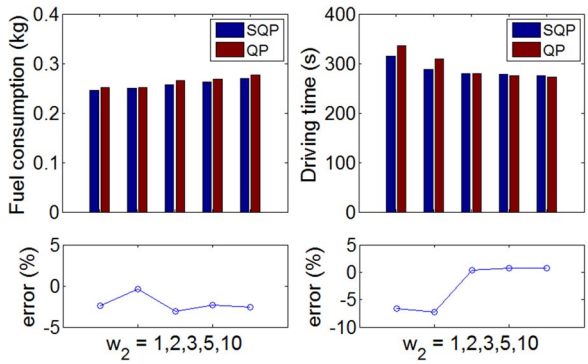

Fig. 7. Comparison of QP results with SQP results for diverse weight values.

First, to confirm the validity of the simplified cost function given in (17), optimization is provided for the original cost function of (15) by using the sequential quadratic programming (SQP) method, and their results are compared. Considering the difference in the orders of the first and second terms of the cost function, the terms are normalized by multiplying the first term by 10^7, which is the difference in the orders of the two terms so that $w_1 = 10^7 \times w_{1(\text{norm})}$. The value of $w_{1(\text{norm})}$ is set to 10, and the value of w_2 is changed from 0.1 to 10, considering their absolute values and variations.

While the original cost function can be minimized by the SQP, its computation time is much longer than that of the simplified cost function provided by the QP method, and it is used only as a benchmark. Computing times of each convergence cycle in the SQP and QP methods for diverse initial conditions and weight values are in the ranges of 80–496 and 9–28 s, respectively, both with an Intel i5-2467M core at a clock speed of 1.6 GHz. Since gear numbers in (13) are fixed during the convergence cycle, this cycle is repeated two to five times to be in accord with the change in the gear numbers owing to the optimized speed profile.

Simulation results for the original cost function produced by the SQP method are shown in Table II. It is shown that the fuel consumption increases and the driving time decreases as the weight on the speed deviation, i.e., w_2, increases. For a w_2 smaller than 1, the speed is lower than the specified speed limits by more than 10%, and the driving time is too long, which is not balanced driving. Thus, only w_2 values equal to or larger than 1 are considered for the optimization.

Fig. 7 compares fuel consumption and driving time using the simplified cost function with the QP method to those using the original cost function with the SQP method. In each panel, the abscissa represents the values of w_2, which are 1, 2, 3, 5, and 10, respectively. Both results show the same tendency for fuel consumption to increase and driving time to decrease as w_2 increases. In the left panel, errors in fuel consumption are in

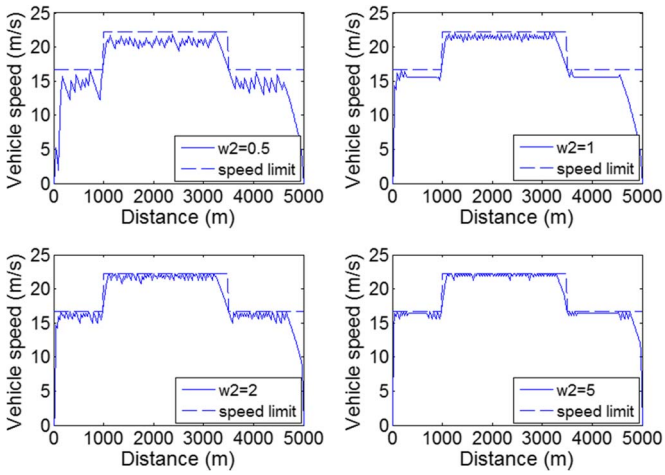

Fig. 8. Resulting speed profiles: speed versus distance.

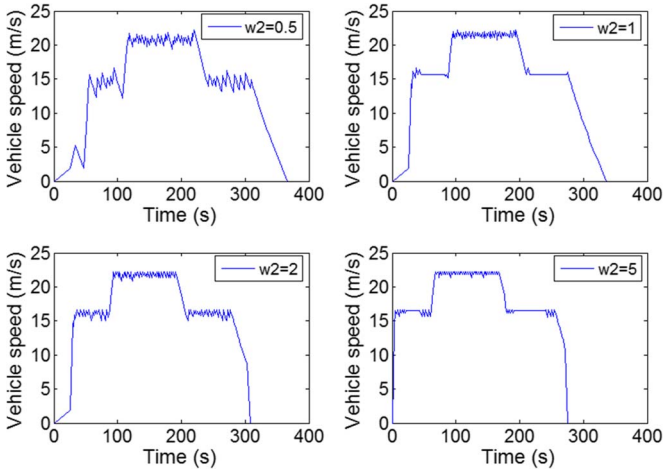

Fig. 9. Resulting speed profiles: time versus speed.

the range of -3.1% to -0.4%. Errors in driving times, which are shown in the right panel, are in the range of -7.3% to 0.7%. The optimization results from the simplified cost function are in good agreement with the results from the original cost function.

Fig. 8 shows the speed profiles generated by the QP method with the simplified cost function for diverse w_1 and w_2 values. It is shown that the speed is kept below that specified by speed limits for a small value of w_2 but that the speed goes closer to the speed limit as w_2 increases.

Fig. 9 shows the speed profiles in a time domain. The speed profile with a smaller w_2 takes a longer driving time, whereas the speed profile with a higher w_2 results in rapid acceleration and deceleration, followed by constant steady-state speeds.

As shown in Figs. 7–9, weighting the fuel consumption leads to a speed profile with a low speed and, accordingly, a long driving time. However, such a low-speed profile is not suitable for actual driving applications, although it consumes less fuel. A vehicle driven at a speed much lower than the speed limit blocks traffic and sometimes increases the probability of car accidents, since the following cars try to change lanes to pass the slow car.

TABLE III
DEPENDENCE OF FUEL CONSUMPTION AND DRIVING TIME ON WEIGHT VALUES

$w_2 = 1$	$w_{1(\mathrm{norm})} = 1$	$w_{1(\mathrm{norm})} = 10$	$w_{1(\mathrm{norm})} = 10^2$
Fuel consumption (kg)	0.253	0.249	0.243
Driving time (s)	309	310	322

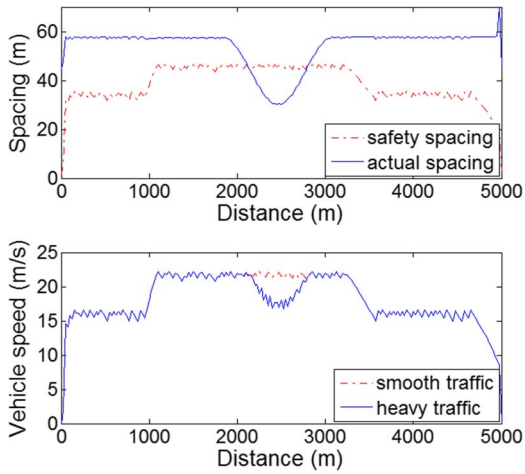

Fig. 10. Example of local adaptation. (a) Safety spacing. (b) Modified speed profile.

In this paper, the average speed deviations from speed limits in the steady-state regions are set to be less than 10% to balance fuel consumption and driving time. This requirement is satisfied when $w_2 \geq 1$. As a reference speed profile, the speed profile obtained in the condition where $w_{1(\mathrm{norm})} = 10$ and $w_2 = 2$ is chosen, which shows the best balance. The fuel consumption and the driving time in this condition are 0.251 kg and 309 s, respectively.

B. Local Adaptation for Traffic Conditions

The local adaptation should be made to follow the target speed quickly and fuel efficiently. How to quickly and fuel efficiently follow the speed is dependent on weights w_1 and w_2 in (24). The terms of the cost function are also normalized by multiplying the first term by 10^4, i.e., $w_1 = 10^4 \times w_{1(\mathrm{norm})}$.

Table III shows the dependence of fuel consumption and driving time on the weight values under smooth traffic conditions. As shown, a large $w_{1(\mathrm{norm})}$ decreases the fuel consumption and increases the driving time. The condition where $w_{1(\mathrm{norm})} = 10$ and $w_2 = 1$ is chosen, which follows the reference speed profile well and exhibits a good balance between fuel and time. Its driving time is longer than the reference speed profile by 1 s, and its fuel consumption is lower by 2 g.

Fig. 10 shows an example of the local adaptation. The upper panel shows that the vehicle encounters heavy traffic in the middle of the driving route. The dotted and solid lines represent the safety spacing required for the reference speed profile and the actual spacing, which means that the spacing is kept when the driver's vehicle follows the reference speed profile, respectively. The spacing to the preceding vehicle is shorter

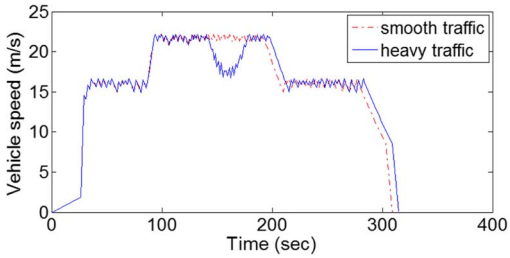

Fig. 11. Locally adapted profile in a time domain.

than the required safety spacing at around a route distance of 2500 m.

In the lower panel, the dotted and solid lines represent the locally adapted speeds under smooth and heavy traffic conditions, respectively. In smooth traffic, the spacing to the preceding vehicle is always wider than the safety spacing, and the vehicle speed follows the reference speed profile well. In heavy traffic, the vehicle speed is slower in the heavy traffic region, i.e., around a route distance of 2500 m, and deviates from the reference speed profile; however, after that region, the vehicle speed follows the reference speed profile again.

Fig. 11 shows the locally adapted speeds in a time domain. It is shown that the adapted speed after the heavy traffic region has the same shape as the reference profile. Thus, for most of the entire driving route, the vehicle can run at reference speeds, which keeps the vehicle running in the optimal condition in the long term if the heavy traffic regions are not too wide. The fuel consumption and the driving time of the heavy traffic speed profile are 0.259 kg and 315 s, respectively, which are larger than those of the smooth condition by 10 g and 5 s, respectively.

If most routes are under heavy traffic conditions, such as rush hour, average speeds at that time and in that region or just before departure may be used as target speeds instead of speed limits. Doing so reduces the number of regions with deviations from the reference speed profile and generates a more realistic long-term optimization result.

V. Discussion and Conclusion

The fuel consumption of a vehicle depends on the characteristics of its drivetrain, road conditions, and traffic conditions. Since it is impossible to predict future traffic conditions accurately before departure, this paper has proposed a distance-based eco-driving scheme using a two-stage hierarchy for long-term optimization and local adaptation.

First, long-term optimization in a distance domain is made for an entire route before departure. Then, while driving, the speed is controlled for only the next location to follow the long-term optimization and to adapt it for traffic conditions.

This distance-based scheme limits the adapted regions to only nearby heavy traffic regions. The reference speed profile is still effective, except in the heavy traffic regions, which means that the vehicle operates in the optimal condition in the long term if the heavy traffic regions are not too wide. This scheme makes its computation time short enough for real-time applications on a long-term optimal basis.

The optimization is provided by the QP method in combination with the simplified fuel rate and vehicle propulsion models. The validity of the simplified models was confirmed by comparing their results with the optimization results provided by the SQP method with the original models.

The time interval corresponding to each distance step and the cost function are simplified to apply the QP method for optimization. Future work involves the long-term optimal strategy, which optimizes the cost function without simplification and has a faster computing time so that diverse driving demands are covered. A finer control for local adaptation is tested for practical and reliable applications. Integration of actual traffic data and the proposed scheme is planned, which makes the proposed scheme more effective.

Acknowledgment

This study was conducted during the sabbatical year of Kwangwoon University in 2015.

References

[1] J. N. Hooker, "Optimal driving for single-vehicle fuel economy," *Transp. Res. A, Gen.*, vol. 22, no. 3, pp. 183–201, May 1988.
[2] W. Y. Chou, Y. C. Lin, Y. H. Lin, and S. Y. Chen, "Intelligent eco-driving suggestion system based on vehicle loading model," in *Proc. ITS Telecommun.*, Taipei, Taiwan, 2012, pp. 558–562.
[3] K. Jakobsen, S. C. H. Mouritsen, and K. Torp, "Evaluating eco-driving advice using GPS/CAN bus data," in *Proc. ACM SIGSPATIAL GIS*, Orlando, FL, USA, 2013, pp. 44–53.
[4] C. Vagg, C. J. Brace, D. Hari, S. Akehurst, J. Poxon, and L. Ash, "Development and field trial of a driver assistance system to encourage eco-driving in light commercial vehicle fleets," *IEEE Trans. Intell. Transp. Syst.*, vol. 14, no. 2, pp. 796–805, Jun. 2013.
[5] S. Park, H. Rakha, K. Ahn, and K. Moran, "Predictive eco-cruise control: Algorithm and potential benefits," in *Proc. IEEE Forum Integr. Sustain. Transp. Syst.*, Vienna, Austria, 2011, pp. 394–399.
[6] T. Schwickart, H. Voos, J. Hadji-Minaglou, and M. Darouach, "An efficient nonlinear model-predictive eco-cruise control for electric vehicles," in *Proc. IEEE Int. Conf. Ind. Informat.*, Bochum, Germany, 2013, pp. 311–316.
[7] T. Schwickart, H. Voos, and M. Darouach, "A real-time implementable model-predictive cruise controller for electric vehicles and energy-efficient driving," in *Proc. IEEE Conf. Control Appl.*, Juan Les Antibes, France, 2014, pp. 617–622.
[8] F. Mensing, R. Trigui, and E. Bideaux, "Vehicle trajectory optimization for application in eco-driving," in *Proc. IEEE VPPC*, Chicago, IL, USA, 2011, pp. 1–6.
[9] Q. Cheng, L. Nouveliere, and O. Orfila, "A new eco-driving assistance system for a light vehicle: Energy management and speed optimization," in *Proc. IEEE IV*, Gold Coast, Qld., Australia, 2013, pp. 1434–1439.
[10] H. T. Luu, L. Nouveliere, and S. Mammar, "Ecological and safe driving assistance system: Design and strategy," in *Proc. IEEE IV*, San Diego, CA, USA, 2010, pp. 129–134.
[11] F. Mensing, E. Bideaux, R. Trigui, and H. Tattegrain, "Trajectory optimization for eco-driving taking into account traffic constraints," *Transp. Res. D, Transp. Environ.*, vol. 18, pp. 55–61, Jan. 2013.
[12] M. A. S. Kamal, M. Mukai, J. Murata, and T. Kawabe, "On board eco-driving system for varying road-traffic environments using model predictive control," in *Proc. IEEE Int. Conf. Control Appl.*, Yokohama, Japan, 2010, pp. 1636–1641.
[13] M. A. S. Kamal, M. Mukai, J. Murata, and T. Kawabe, "Ecological vehicle control on roads with up–down slopes," *IEEE Trans. Intell. Transp. Syst.*, vol. 12, no. 3, pp. 783–794, Sep. 2011.
[14] J. Jing, "Vehicle fuel consumption optimization using model predictive control based on V2V communication," M.S. thesis, Dept. Electron. Comput. Sci., Ohio State Univ., Columbus, OH, USA, 2014.
[15] S. Xu, K. Deng, S. E. Li, S. Li, and B. Cheng, "Legendre pseudo-spectral computation of optimal speed profiles for vehicle eco-driving system," in *Proc. IEEE Intell. Veh. Symp.*, Dearborn, MI, USA, 2014, pp. 1103–1108.

[16] T. Choe, A. Skabardonis, and P. Varaiya, "Freeway Performance Measurement System (PeMS): An operational analysis tool," Univ. California, Berkeley, CA, USA, Jan. 2001.
[17] "PeMS," California Dept. Transp., Sacramento, CA, USA. [Online]. Available: http://pems.dot.ca.gov
[18] N. J. Kohut, J. K. Hedrick, and F. Borrelli, "Integrating traffic data and mode predictive control to improve fuel economy," in *Proc. 12th IFAC Symp. Control Transp. Syst.*, Redondo Beach, CA, USA, 2009, pp. 155–160.
[19] M. A. S. Kamal, M. Mukai, J. Murata, and T. Kawabe, "Model predictive control of vehicles on urban roads for improved fuel economy," *IEEE Trans. Control Syst. Technol.*, vol. 21, no. 3, pp. 831–841, May 2013.
[20] G. D. Nunzio, C. C. D. Wit, P. Moulin, and D. D. Domenico, "Eco-driving in urban traffic networks using traffic signal information," in *Proc. IEEE Conf. Decision Control*, Florence, Italy, 2013, pp. 892–898.
[21] C. Sun, S. H. Moura, X. Hu, J. K. Hedrick, and F. Sun, "Dynamic traffic feedback data enabled energy management in plug-in hybrid electric vehicles," *IEEE Trans. Control Syst. Technol.*, vol. 23, no. 3, pp. 1075–1086, May 2015.
[22] Q. Gong, Y. Li, and Z. R. Peng, "Trip based power management of plug-in hybrid electric vehicle with two-scale dynamic programming," in *Proc. IEEE Veh. Power Propulsion Conf.*, Arlington, TX, USA, 2007, pp. 12–19.
[23] H. Borhan, A. Vahidi, A. M. Phillips, M. L. Kuang, I. V. Kolmanovsky, and S. D. Cairano, "MPC based energy management of a power-split hybrid electric vehicle," *IEEE Trans. Control Syst. Technol.*, vol. 20, no. 3, pp. 293–603, May 2012.
[24] Y. Guo, J. Xiong, S. Xu, and W. Su, "Two-stage economic operation of microgrid-like electric vehicle parking deck," *IEEE Trans. Smart Grid*, vol. 7, no. 3, pp. 1703–1712, May 2016.
[25] Q. Gong, Y. Li, and Z. R. Peng, "Optimal power management of plug-in HEV with intelligent transportation system," in *Proc. IEEE/ASME Int. Conf. Adv. Intell. Mechatron.*, Zürich, Switzerland, 2007, pp. 1–6.
[26] Y. Chen, X. Li, C. Wiet, and J. Wang, "Energy management and driving strategy for in-wheel motor electric ground vehicles with terrain profile preview," *IEEE Trans. Ind. Informat.*, vol. 10, no. 3, pp. 1938–1947, Aug. 2014.
[27] "Autonomie," Argonne Nat. Lab., Lemont, IL, USA. [Online]. Available: http://www.autonomie.net
[28] N. Kim, A. Rousseau, and E. Rask, "Autonomie model validation with test data for 2010 Toyota Prius," in *Proc. SAE*, Detroit, MI, USA, 2012, pp. 1–14.
[29] N. Kim, M. Duoba, N. Kim, and A. Rousseau, "Validating Volt PHEV model with dynamometer test data using Autonomie," *SAE Int. J. Passenger Cars*, vol. 6, no. 2, pp. 985–992, 2013.
[30] G. Rizzoni, L. Guzzella, and B. M. Baumann, "Unified modeling of hybrid electric vehicle drivetrains," *IEEE Trans. Mechatron.*, vol. 4, no. 3, pp. 246–257, Sep. 1999.
[31] Z. Chen and C. Mi, "Power management of PHEV using quadratic programming," *Int. J. Elect. Hybrid Veh.*, vol. 3, no. 3, pp. 246–258, 2011.
[32] Z. Zhou, C. C. Mi, R. Xiong, J. Xu, and C. You, "Energy management of a power-split plug-in hybrid electric vehicle based on genetic algorithm and quadratic programming," *J. Power Sources*, vol. 248, pp. 416–426, 2014.
[33] Y. Yang, X. Hu, H. Pei, and Z. Peng, "Comparison of power-split and parallel hybrid powertrain architectures with a single electric machine: Dynamic programming approach," *Appl. Energy*, vol. 168, pp. 683–690, 2016.

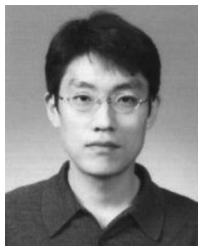

Hansang Lim (M'09) received the B.S., M.S., and Ph.D. degrees from Seoul National University, Seoul, South Korea, in 1996, 1998, and 2004, respectively.

From 2004 to 2007, he was with the Telecommunication R&D Center, Samsung Electronics Company, Ltd. He is currently an Associate Professor with the Department of Electronics Convergence Engineering, Kwangwoon University, Seoul, and a Visiting Scholar with the Department of Electrical and Computer Engineering, University of Michigan, Dearborn, MI, USA. His research interests include instrumentation and measurement systems, power supply and distribution systems, and vehicular electronics.

Wencong Su (S'06–M'13) received the B.S. degree (with distinction) from Clarkson University, Potsdam, NY, USA, in 2008; the M.S. degree from Virginia Polytechnic Institute and State University, Blacksburg, VA, USA, in 2009; and the Ph.D. degree from North Carolina State University, Raleigh, NC, USA, in 2013, all in electrical engineering.

He is currently an Assistant Professor with the Department of Electrical and Computer Engineering, University of Michigan, Dearborn, MI, USA. His research interests include power and energy systems, electrified transportation systems, cyberphysical systems, and electricity markets.

Chunting Chris Mi (S'00–A'01–M'01–SM'03–F'12) received the B.S.E.E. and M.S.E.E. degrees from Northwestern Polytechnical University, Xi'an, China, and the Ph.D. degree from the University of Toronto, Toronto, ON, Canada, all in electrical engineering.

He is currently a Professor of electrical and computer engineering and the Director of the Department of Energy (DOE)-funded Graduate Automotive Technology Education Center for Electric Drive Transportation with San Diego State University, San Diego, CA, USA. Prior to joining San Diego State University in 2015, he was with General Electric Company, Peterborough, ON, and a Professor with the Department of Electrical and Computer Engineering, University of Michigan, Dearborn, MI, USA. He has conducted extensive research and has authored or coauthored over 100 journal papers. His research interests include electric drives, power electronics, electric machines, renewable energy systems, and electrical and hybrid vehicles.

Dr. Mi is an Area Editor of the IEEE TRANSACTIONS ON VEHICULAR TECHNOLOGY and an Associate Editor of the IEEE TRANSACTIONS ON POWER ELECTRONICS and the IEEE TRANSACTIONS ON INDUSTRY APPLICATIONS.